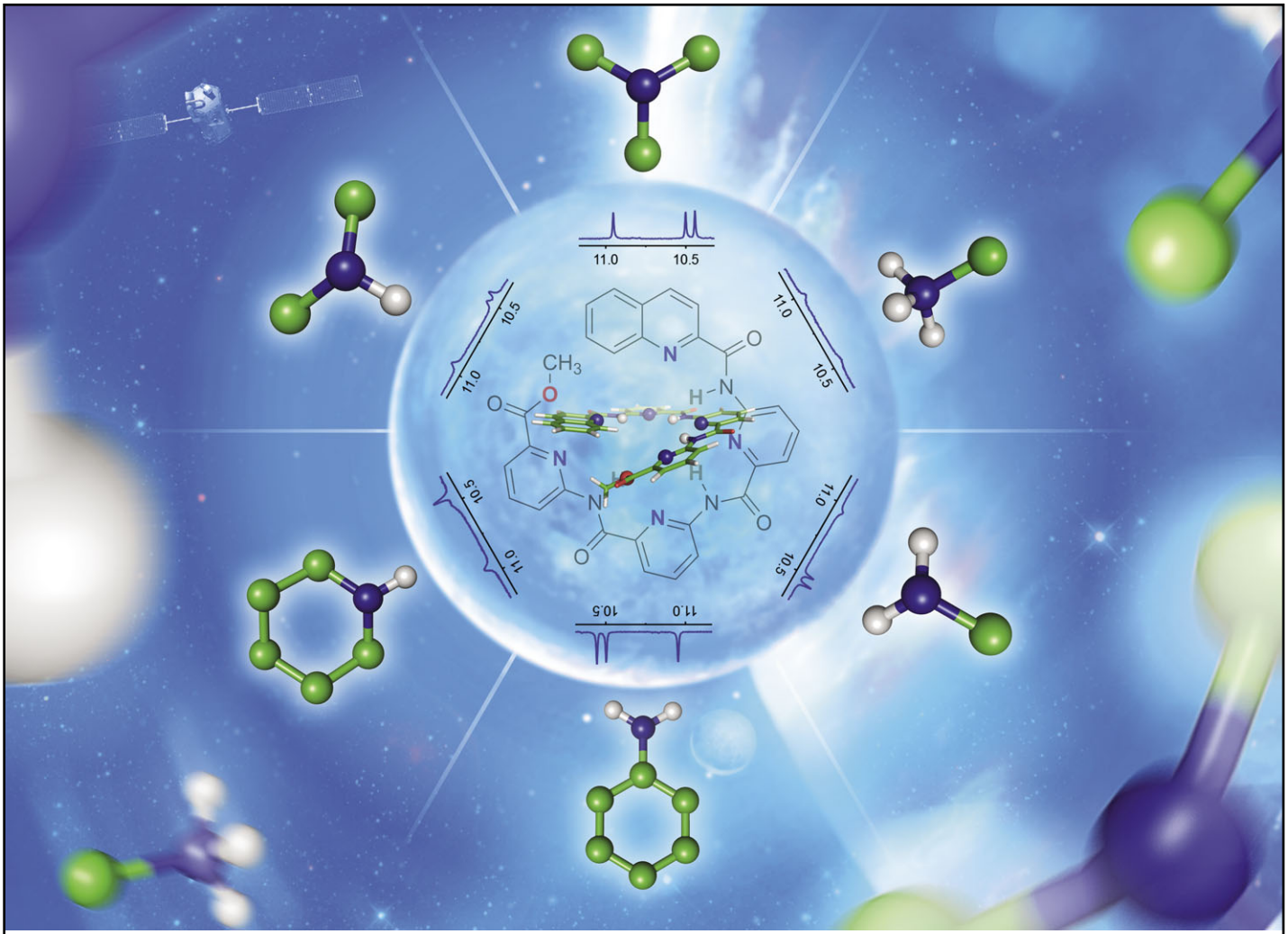

Showcasing research from the laboratory of Professor Huaqiang Zeng, Department of Chemistry at the National University of Singapore.

Patterned recognitions of amines and ammonium ions by a pyridine-based helical oligoamide host

In response to binding to amine and ammonium guests of varying types, a pyridine-based folding oligomer displays fingerprint regions in its ^{1}H NMR spectra that allow for the easy identification and classification of the bound guests.

As featured in:

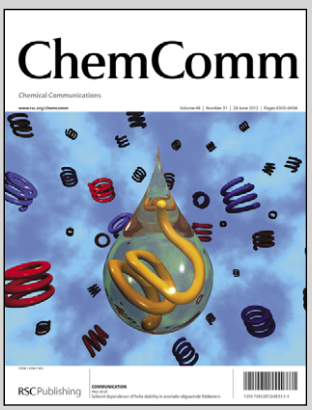

See Huaqiang Zeng *et al.*, *Chem. Commun.*, 2012, **48**, 6343.

RSC Publishing

www.rsc.org/chemcomm

Registered Charity Number 207890

ChemComm

Dynamic Article Links

Cite this: *Chem. Commun.*, 2012, **48**, 6343–6345

www.rsc.org/chemcomm

COMMUNICATION

Patterned recognition of amines and ammonium ions by a pyridine-based helical oligoamide host†

Wei Qiang Ong,[a] Huaiqing Zhao,[a] Chang Sun,[a] Ji'En Wu,[a] Zicong Wong,[a] Sam F. Y. Li,[a] Yunhan Hong[b] and Huaqiang Zeng*[a]

Received 31st December 2011, Accepted 20th March 2012
DOI: 10.1039/c2cc18182g

In response to binding to amine and ammonium guests of varying types, a pyridine-based folding oligomer displays fingerprint regions in its ^{1}H NMR spectra that allow for the easy identification and classification of the bound guests.

Selective recognition of amine and ammonium guests is a considerably challenging issue particularly when given Nature's high selectivity towards ammonia sensing by using simple organic or inorganic building blocks.[1] For example, several reported organic and coordination receptors capable of sensing amines are unable to efficiently differentiate amines of varying types, and amines from ammonium ions.[2] Effective recognition and differentiation of amines or ammonium ions is valuable not only in environmental and industrial monitoring but also for food quality control and clinical disease diagnosis.[3] On the other hand, aromatic foldamers of diverse structures have been elaborated over the recent years.[4] A wealth of functions derived from these folding backbones have also been demonstrated.[5] However, aromatic foldamers capable of recognizing functional groups as simple as amines or ammonium cations appear to be very rare. This communication demonstrates the functional utility of pyridine-based foldamers such as tetramer **1** (Fig. 1a) as the host for various amine and ammonium guests, exhibiting differential binding patterns for easy detection and classification by using the corresponding ^{1}H NMR fingerprint regions.

We recently reported a series of pyridine-based foldamers with their folded structures enforced by internally placed continuous H-bonding networks.[5g,h,6] Results have shown that this new set of backbone-rigidified pyridine-based folding oligoamides requires ~four repeating units to form a helical turn. The cavity enclosed by these pyridine foldamers is ~2.5 Å in radius, and is decorated by both H-bond donors (amide protons) and acceptors (pyridine N-atoms and ester O-atoms), making these pyridine foldamers potentially suitable for accommodating the amine or ammonium groups (Fig. 1a).

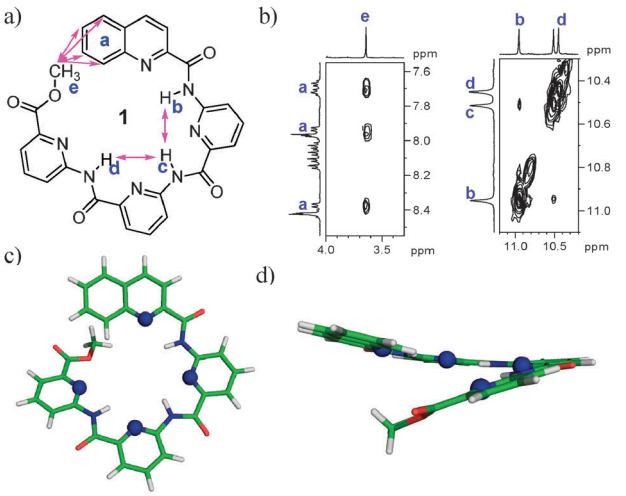

Fig. 1 (a) NOE contacts in **1**, illustrated by double headed pink arrows. (b) Expanded 2D NOESY spectra of **1** ($CDCl_3$, 500 MHz, 300 K, mixing time = 0.5 s), showing NOE contacts among amide protons b, c and d and end-to-end NOE contacts among methyl protons e and aromatic protons a. (c) Top and (d) side views of *ab initio* optimized structure of **1** at the level of B3LYP/6-31G*.

1 was synthesized in 7 steps using a step-by-step approach with an overall yield of about 32% (Scheme S1, ESI†). The crescent-shaped structure in **1** is evidenced by the experimentally observed NOE contacts between amide protons c and b or d and by the end-to-end NOE contacts between the end methoxy protons e and protons a of the quinoline moiety (Fig. 1b). Its helical geometry can be reliably established by the *ab initio* calculation using density functional theory at the B3LYP/6-31G* level (Fig. 1c and d),[7] and by the crystal structures of analogous pyridine oligoamides that take up a helical conformation starting from tetramers that contain bulkier end groups such as an ester group.[4] Such a helical geometry in **1** is also in agreement with the above NOE results.

Using the soft electrospray ionization (ESI) method in a high resolution format, the molecular ion peaks that represent each of the host–guest complexes in a 1 : 1 ratio were obtained with some representative aliphatic amine and ammonium guests (Table 1), confirming the formation of the host–guest complexes in a 1 : 1 ratio and their identities (Table 1).†

[a] *Department of Chemistry, National University of Singapore, Singapore 117543. E-mail: chmzh@nus.edu.sg; Tel: +65-6516-2683*
[b] *Department of Biological Sciences, National University of Singapore, 14 Science Drive 4, Singapore 117543*

† Electronic supplementary information (ESI) available: Synthetic procedures and a full set of characterization data including ^{1}H/^{13}C NMR, HRMS, 2D NOESY, and molecular modelling. See DOI: 10.1039/c2cc18182g

Table 1 List of amine and ammonium guests studied and the m/z of the [**1**·guest] complexes determined using high-resolution mass spectroscopy

S/N	Guest	Measured m/z[a]	Molecular ion
Primary amine			
1	Isopropylamine	607.2440	$[\mathbf{1}\cdot C_3H_7NH_2 + H]^+$
2	1-Aminooctane	677.3218	$[\mathbf{1}\cdot C_8H_{17}NH_2 + H]^+$
3	1,8-Diaminooctane	692.3311	$[\mathbf{1}\cdot C_8H_{16}(NH_2)_2 + H]^+$
4	2,2′-(Ethylenedioxy)-bis(ethylamine)	696.2878	$[\mathbf{1}\cdot C_6H_{12}O_2(NH_2)_2 + H]^+$
Acyclic secondary amine			
5	Di-*n*-propylamine	649.2891	$[\mathbf{1}\cdot (C_3H_7)_2NH + H]^+$
6	Di-*n*-hexylamine	733.3848	$[\mathbf{1}\cdot (C_6H_{13})_2NH + H]^+$
7	Di-*n*-octylamine	789.4458	$[\mathbf{1}\cdot (C_8H_{17})_2NH + H]^+$
Cyclic secondary amine			
8	Azetidine	605.2265	$[\mathbf{1}\cdot C_3H_6NH + H]^+$
9	Pyrrolidine	619.2413	$[\mathbf{1}\cdot C_4H_8NH + H]^+$
10	Piperidine	633.2578	$[\mathbf{1}\cdot C_5H_{10}NH + H]^+$
Tertiary amine			
11	Triethylamine	649.2885	$[\mathbf{1}\cdot (C_2H_5)_3N + H]^+$
12	Diisopropylethylamine	677.3224	$[\mathbf{1}\cdot C_8H_{19}N + H]^+$
13	1-Methylpiperidine	647.2752	$[\mathbf{1}\cdot C_6H_{13}N + H]^+$
Aromatic amine			
14	Aniline	Not detected	
Ammonium salts			
15	1-Octylammonium perchlorate	677.3212	$[\mathbf{1}\cdot C_8H_{17}NH_3]^+$
16	Di-*n*-octylammonium perchlorate	789.4469	$[\mathbf{1}\cdot (C_8H_{17})_2NH_2]^+$

[a] HRMS obtained by using ESI method.

Titrating **1** at 2 mM in "normal" $CDCl_3$ directly taken from the bottle using various guests in varying equivalents does not lead to noticeable changes in the chemical shift for all the three amide protons b–d of **1** (Fig. 2 and Fig. S4–S21, ESI†), indicating the minimal interference guest binding has on the high strength

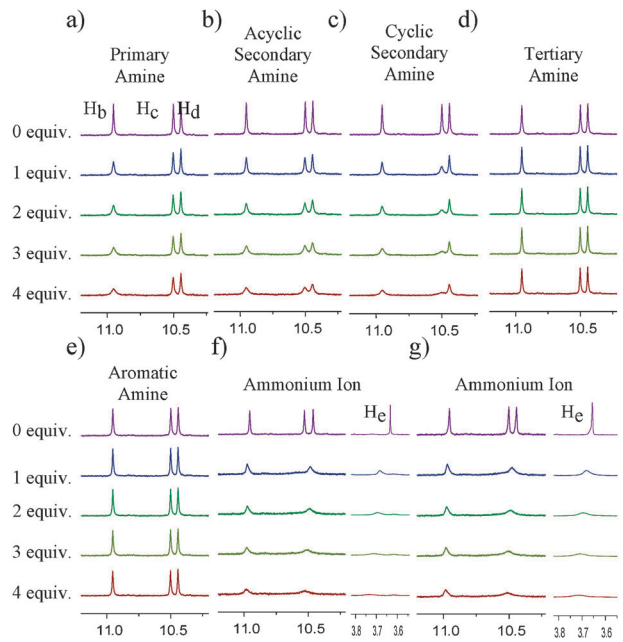

Fig. 2 Representative ^{1}H NMR (2 mM, $CDCl_3$) fingerprint regions for amide protons b–d and ester methyl protons e of **1** in the presence of up to four equivalents of (a) 1-octylamine, (b) di-*n*-octylamine, (c) piperidine, (d) triethylamine, (e) aniline, (f) 1-octylammonium perchlorate and (g) di-*n*-octylammonium perchlorate.

intramolecular hydrogen-bonding network in **1** and on its helical structure. Selected 2D NOESY experiments on the 1 : 1 mixture of **1** and octylamine or piperidine reveal the presence of strong NOE contacts among amide protons of **1** that are indicative of the persistence of its folded structure (Fig. S2 and S3, ESI†).

With the addition of increasing amounts of the amine guests excluding tertiary and aromatic amines, the intensity or the height of the NMR peaks for the amide protons progressively decreased, and in most cases, the affected peaks also became broadened (Fig. 2). Possibly, this occurs as a result of binding-induced changes in the spin–spin relaxation time of amide protons that interact with amine or ammonium protons in varying strengths, altering both the intensity and shape of the NMR peaks. Except for tertiary amines (Fig. 2d and Fig. S16–S18, ESI†) that contain no protons and aromatic amines (Fig. 2e and Fig. S19, ESI†) that are weak in basicity and thus do not elicit any change in NMR signals, a few general patterns can be identified for primary and secondary amines as well as ammonium cations.

For primary amines, it was observed that amide proton b was perturbed most as compared to the other two amide protons c and d that remained very sharp throughout the titrations (Fig. 2a and Fig. S6–S9, ESI†). It is highly likely that this is due to the stronger binding of proton b than protons c and d with primary amines. To assess this possibility, a series of possible structures for the complex **1**·methylamine were optimized at the level of B3LYP/6-31G//6-311G+(2d,p). Expectedly, our calculations show that the most stable complex formed between **1** and methylamine indeed is the one where the amine sits in the cavity of **1** with the amine N-atom forming a strong H-bond (1.84 Å) with amide proton b in **1** (Fig. 3a), making proton b experience the strongest influence of primary amines during the ^{1}H NMR titration experiments. The computational results also show that placing methylamine on either side of **1** leads to energetically almost equivalent **1**·methylamine complexes with the "bottom" complex being 0.4 kcal mol^{-1} more favored (Fig. 3a).

In the case of acyclic secondary amines, all the three amide protons b–d become increasingly broadened roughly to an equal extent (Fig. 2b and Fig. S10–S12, ESI†). Taking dimethylamine as the test compound for *ab initio* calculations, the most stable complex shown in Fig. 3b actually has the methyl group and the amine N-atom from dimethylamine forming weak intermolecular H-bonds of 2.52 Å and 2.40 Å with the ester O-atom and the ester methyl proton from **1**, respectively, and no medium or strong H-bonds are found

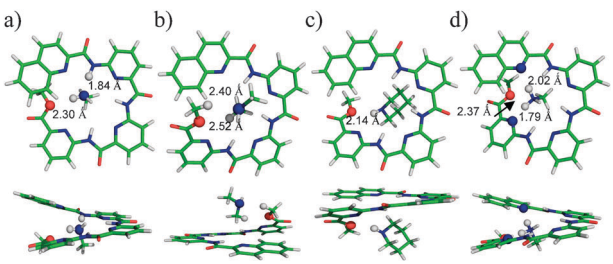

Fig. 3 Top and side views of the computationally determined most stable complex formed between **1** and (a) methylamine, (b) dimethylamine, (c) piperidine and (d) methylammonium cation at the B3LYP/6-31G//6-311G+(2d,p) level. Atoms involved in intermolecular H-bonds of varying lengths are represented as small balls (gray = H, red = O and blue = N). See Fig. 1a for the assignment of amide protons b–d.

between dimethylamine and **1**. The weakly interacting acyclic secondary amines therefore exert unbiased influences over the three amide protons b–d. Interestingly, a slightly different trend was observed for cyclic secondary amines where proton c becomes the most broadened and starts disappearing in the presence of four equivalents of amine guests while the NMR peaks for protons b and d are altered by both acyclic and cyclic secondary amines almost to equal extents (Fig. 2c and Fig. S13–S15, ESI†). Computationally, the cyclic secondary amine (*i.e.* piperidine, Fig. 3c) interacts almost perpendicularly with **1**. The amine NH proton in piperidine forms a strong H-bond of 2.14 Å with the ester O-atom of **1** and a weak H-bond of 2.88 Å with the pyridine N-atom of **1**. On average, the protons from the ring atoms of piperidine are closer to amide protons b and c ($\sim$2.6 Å) than to proton d ($>$3.3 Å). These electrostatic interactions among the protons may modify the electron density around protons b and c, possibly resulting in the observed titration pattern of ^{1}H NMR peaks where the amide protons b and c are affected more than proton d by cyclic secondary amines (Fig. 2c).

Lastly, the addition of ammonium ions into **1** leads to line broadenings and a rapid decrease in the size of ^{1}H NMR peaks for all the three amide protons (Fig. 2f and g and Fig. S20 and S21, ESI†). Unseen for primary, secondary and tertiary amines, ammonium ions additionally exhibit a dramatic influence over the size and shape of the ester methyl peaks (Fig. 2f and g and Fig. S20 and S21, ESI†).

It is known that "normal" $CDCl_3$ slowly decomposes upon prolonged storage to produce trace amounts of DCl that may protonate the amines or **1** to varying extents. To probe the possible effect of DCl, the above ^{1}H NMR-based analyses were re-carried out in "neutralized" $CDCl_3$ filtered with basic alumina. For all the different types of amines studied, the fingerprint regions identical to those shown in Fig. 2a–e were obtained (Fig. S5a–e, ESI†). For primary ammonium salts, the broadening and disappearance of both amide and ester peaks take place with addition of 10, rather than 4, equivalents of ammonium salts (Fig. S5f, ESI†).[8] Interestingly, addition of up to 12 equivalents of secondary ammonium ions only leads to a slight decrease in peak height with no observation of line broadening and disappearance, suggesting that the combined use of "normal' and "neutralized" $CDCl_3$ allows for a further differentiation between primary and secondary ammonium ions.

While tetramer **1** displays up to six differential ^{1}H NMR-based patterns toward amines and ammonium ions (Fig. 2 and Fig. S5, ESI†), similar analyses on shorter oligomers show that both dimer **1b** (Fig. S22, ESI†) and trimer **1d** (Fig. S23, ESI†) exhibit much less degenerated patterns. It is worthy to note that primary and secondary ammonium ions also can be confidently discriminated by both **1b** and **1d**. By combining with **1**, **1b** further allows for the unambiguous differentiation of primary from secondary amines.

The above observations from the ^{1}H NMR experiments illustrate that varying amine and ammonium guests each displays a differential binding mode with host **1**. By comparing ^{1}H NMR fingerprint regions involving the amide protons and the ester methyl group in **1** and aided further by dimer **1b** and trimer **1d**, one could possibly distinguish among various types of amines, between ammonium ions, and between amine and ammonium guests.

Financial support to H.Z. by National Research Foundation Competitive Research Programme Grant (R-154-000-529-281), NUS AcRF Tier 1 grant (R-143-000-419-646) and Environment and Water Industry Development Council and Economic Development Board (SPORE, COY-15-EWI-RCFSA/N197-1) is gratefully acknowledged.

Notes and references

1 S. Khademi, J. O'Connell, III, J. Remis, Y. Robles-Colmenares, L. J. W. Miercke and R. M. Stroud, *Science*, 2004, **305**, 1587.

2 (*a*) P. L. McGrier, K. M. Solntsev, J. Schonhaber, S. M. Brombosz, L. M. Tolbert and U. H. F. Bunz, *Chem. Commun.*, 2007, 2127; (*b*) M. R. Ajayakumar and P. Mukhopadhyay, *Chem. Commun.*, 2009, 3702; (*c*) C.-F. Chow, H.-K. Kong, S.-W. Leung, B. K. W. Chiu, C.-K. Koo, E. N. Y. Lei, M. H. W. Lam, W.-T. Wong and W.-Y. Wong, *Anal. Chem.*, 2010, **83**, 289; (*d*) S. M. A. Pinto, M. A. O. Lourenço, M. J. F. Calvete, A. R. Abreu, M. T. S. Rosado, H. D. Burrows and M. M. Pereira, *Inorg. Chem.*, 2011, **50**, 7916; (*e*) C. G. Sun, Q. Lin and N. Y. Fu, *Chin. Chem. Lett.*, 2012, **23**, 217.

3 (*a*) W.-L. Gong, K. J. Sears, J. E. Alleman and E. R. Blatchley III, *Environ. Toxicol. Chem.*, 2004, **23**, 239; (*b*) Y. Takagai, Y. Nojiri, T. Takase, W. L. Hinze, M. Butsugan and S. Igarashi, *Analyst*, 2010, **135**, 1417.

4 For reviews on foldamers, see: (*a*) S. H. Gellman, *Acc. Chem. Res.*, 1998, **31**, 173; (*b*) I. Huc, *Eur. J. Org. Chem.*, 2004, 17; (*c*) B. Gong, *Acc. Chem. Res.*, 2008, **41**, 1376; (*d*) I. Saraogi and A. D. Hamilton, *Chem. Soc. Rev.*, 2009, **38**, 1726; (*e*) X. Zhao and Z. T. Li, *Chem. Commun.*, 2010, **46**, 1601. For pioneering works on using H-bonds to rigidify aromatic backbones, see: (*f*) Y. Hamuro, S. J. Geib and A. D. Hamilton, *Angew. Chem., Int. Ed.*, 1994, **33**, 446; (*g*) V. Berl, I. Huc, R. G. Khoury, M. J. Krische and J. M. Lehn, *Nature*, 2000, **407**, 720; (*h*) J. Zhu, R. D. Parra, H. Q. Zeng, E. Skrzypczak-Jankun, X. C. Zeng and B. Gong, *J. Am. Chem. Soc.*, 2000, **122**, 4219; (*i*) V. Berl, I. Huc, R. Khoury and J.-M. Lehn, *Chem.–Eur. J.*, 2001, **7**, 2798.

5 For cation-binding by pentamers, see: (*a*) B. Qin, C. L. Ren, R. J. Ye, C. Sun, K. Chiad, X. Y. Chen, Z. Li, F. Xue, H. B. Su, G. A. Chass and H. Q. Zeng, *J. Am. Chem. Soc.*, 2010, **132**, 9564; (*b*) C. L. Ren, V. Maurizot, H. Q. Zhao, J. Shen, F. Zhou, W. Q. Ong, Z. Y. Du, K. Zhang, H. B. Su and H. Q. Zeng, *J. Am. Chem. Soc.*, 2011, **133**, 13930. For binding of organic cationic species, see: (*c*) A. R. Sanford, L. Yuan, W. Feng, K. Yamato, R. A. Flowers and B. Gong, *Chem. Commun.*, 2005, 4720. For water binding, see: (*d*) R. M. Meudtner and S. Hecht, *Angew. Chem., Int. Ed.*, 2008, **47**, 4926; (*e*) J.-M. Suk, V. R. Naidu, X. Liu, M. S. Lah and K.-S. Jeong, *J. Am. Chem. Soc.*, 2011, **133**, 13938. For anion recognition, see: (*f*) J. Garric, J.-M. Leger and I. Huc, *Angew. Chem., Int. Ed.*, 2005, **44**, 1954; (*g*) W. Q. Ong, H. Q. Zhao, X. Fang, S. Woen, F. Zhou, W. L. Yap, H. B. Su, S. F. Y. Li and H. Q. Zeng, *Org. Lett.*, 2011, **13**, 3194; (*h*) H. Q. Zhao, W. Q. Ong, X. Fang, F. Zhou, M. N. Hii, S. F. Y. Li, H. B. Su and H. Q. Zeng, *Org. Biomol. Chem.*, 2012, **10**, 1172. For DNA G-quadruplex stabilizers, see: (*i*) P. S. Shirude, E. R. Gillies, S. Ladame, F. Godde, K. Shin-Ya, I. Huc and S. Balasubramanian, *J. Am. Chem. Soc.*, 2007, **129**, 11890. For ion transporter, see: (*j*) A. J. Helsel, A. L. Brown, K. Yamato, W. Feng, L. H. Yuan, A. J. Clements, S. V. Harding, G. Szabo, Z. F. Shao and B. Gong, *J. Am. Chem. Soc.*, 2008, **130**, 15784.

6 W. Q. Ong, H. Q. Zhao, Z. Y. Du, J. Z. Y. Yeh, C. L. Ren, L. Z. W. Tan, K. Zhang and H. Q. Zeng, *Chem. Commun.*, 2011, **47**, 6416.

7 (*a*) B. Qin, X. Y. Chen, X. Fang, Y. Y. Shu, Y. K. Yip, Y. Yan, S. Y. Pan, W. Q. Ong, C. L. Ren, H. B. Su and H. Q. Zeng, *Org. Lett.*, 2008, **10**, 5127; (*b*) Y. Yan, B. Qin, Y. Y. Shu, X. Y. Chen, Y. K. Yip, D. W. Zhang, H. B. Su and H. Q. Zeng, *Org. Lett.*, 2009, **11**, 1201; (*c*) Y. Yan, B. Qin, C. L. Ren, X. Y. Chen, Y. K. Yip, R. J. Ye, D. W. Zhang, H. B. Su and H. Q. Zeng, *J. Am. Chem. Soc.*, 2010, **132**, 5869.

8 In the computed structure that has a very high binding energy of 30.55 kcal mol^{-1}, the primary ammonium ion is slightly nearer to the ester side, forming strong H-bonds with **1** (1.79, 2.02 and 2.37 Å, Fig. 3d). In this case, our surmise is that the ammonium ion possibly alters the NMR signals *via* chemical exchange involving ammonium protons and protons from amide and ester groups of **1** by virtue of forming a highly stable complex. The presence of DCl apparently accelerates the exchange process, leading to much faster line broadening and disappearance as seen in Fig. 2f when "normal" $CDCl_3$ was used.